

CORRELATIONS OF DEFLECTION ANGLES OF A LASER BEAM IN A HOT TURBULENT JET OF AIR: THEORETICAL DETERMINATION AND EXPERIMENTAL MEASUREMENT OF THE STRUCTURE COEFFICIENT OF REFRACTIVE INDEX FLUCTUATIONS

J. Bilong II¹, E. Ngo Nyobe², J. Hona¹, and E. Pemha^{1, *}

¹Applied Mechanics Laboratory, Faculty of Science, University of Yaoundé I, P. O. Box 7389, Yaoundé, Cameroon

²Department of Mathematics and Physical Science, National Advanced School of Engineering, University of Yaoundé I, P. O. Box 8390, Yaoundé, Cameroon

Abstract—Using the geometrical optics approximation, a theoretical prediction of the deflection angle correlation of a laser beam propagating in a hot turbulent jet is found as a functional form of the turbulent spectrum of the refractive index fluctuations. By applying the modified Von Karman model and Tatarskii model, the structure coefficient of the refractive index and the deflection angle correlation of the laser beam are then computed by means of a numerical procedure. Experiments to measure the structure coefficient are performed. A good agreement between the experimental results obtained and the theoretical predictions demonstrates the validity of the theoretical approach.

1. INTRODUCTION

The propagation of light in turbulent media has been the subject of research for the past forty years, notably for the cases in which the turbulent medium considered is the atmosphere [1–3]. This topic is of an increasing interest because of the important role of laser beams in a wide range of modern technological applications, such as electromagnetic transmissions [4] in optical systems and in the atmosphere [5], satellite communication [6], medical diagnostics [7–10], and diagnostic techniques of turbulence [11] in heated turbulent media and in combustion chambers.

Received 9 May 2012, Accepted 31 July 2012, Scheduled 2 August 2012

* Corresponding author: Elkana Pemha (elkanaderbeau@yahoo.fr).

When a laser beam is sent into a heated turbulent medium, the refractive index in the medium undergoes random fluctuations called optical turbulence induced by the temperature fluctuations in the medium. This causes random deflections of the laser beam, generates random phase modulations in the laser beam wave front, and then creates random fluctuations of the light wave amplitude by the diffraction process. Many papers have been devoted to the study of phase and intensity fluctuations of the laser beam in random media [12] and other studies have been carried out the possibility of using the fractional moments [13], or the methods for solving the parabolic equation of moments [14]. It is well known that the directional fluctuations of the laser beam are more suitable for studying turbulence because they are very sensitive to turbulence inhomogeneities. Consequently, many scientists [15–17] are making increasing use of information coming from deflection angle fluctuations of laser beams inside turbulent media to extract information about turbulence. In our previous investigations [18–22], we have done works in connection with the angular fluctuations of laser beams in random media. More precisely, the angle-of-arrival probability density of a laser beam in a strong plane-flame turbulence has been determined theoretically and experiments have been performed to confirm theoretical results [18]. The diffusion coefficient of a heated air stream which is correlated to the deflection angle fluctuations of a laser beam has been determined using an optical technique coupled with an optimization approach [19, 20]; for the same jet, the stochastic properties of the random direction of a laser beam have been studied [21]. The temporal spectrum of the laser beam angle-of-arrival is measured by means of an experimental technique which utilizes an interference pattern to separate directional fluctuations of the laser beam [22]. More recently [11], a genetic algorithm technique based on the directional fluctuations of a laser beam in a hot turbulent jet of air has been performed for the extraction of local information about thermal turbulence in the jet without introducing any probe into the flow.

In this paper, we study the correlations of the deflection angle fluctuations of a single laser beam propagating through a hot turbulent jet of air. The theory we elaborate is the same for any random medium. To obtain some results, we assume the experimental conditions we have applied in our previous works for the hot turbulent jet of air, which we have considered as the turbulent medium. The results presented in this paper will be used later to extract information on turbulence in the jet, using the correlations of deflection angles of the laser beam. For a better understanding of this work, the rest of this paper consists of six

sections. In Section 2, the problem under study is stated. Section 3 is devoted to the theoretical approach we have developed to determine the correlation functions of the laser beam deflection angles, in terms of the correlations of refractive index fluctuations. In Section 4, the completed theoretical results are obtained by applying the models of turbulence spectrum, notably the Karman and Tatarskii models. The numerical procedure we have applied is described in Section 5: by using the value of the diffusion coefficient published in a previous paper, the structure coefficient of the refractive index fluctuations is computed and the values of the deflection angle correlation of the laser beam are deduced. In Section 6, experiments which enable to measure the structure coefficient are performed and a good agreement between the experimental measurements and the theoretical results is observed. Conclusion is given in the last Section.

2. STATEMENT OF THE PROBLEM

Let us consider a single laser beam which propagates through a hot turbulent jet of air. To study the propagation of the laser beam, we define a Cartesian coordinate system with three unit vectors (\mathbf{x} , \mathbf{y} , \mathbf{z}). The x axis is the unperturbed direction of the laser beam, that is, its direction before entering into the turbulent medium; and the plane (y , z) is perpendicular to the x axis. When investigating the properties of the fluctuations of the laser beam deflection angles or studying any stochastic process in connection with the directional fluctuations of the laser beam in a turbulent medium, one has to study the phase fluctuations of the laser beam, or apply the geometrical optics approximation [23] used here. We assume that the laser beam remains sufficiently narrow along its whole path such that the diffraction effects are negligible compared to the refraction effects. This occurs when the following four conditions are met [18–22]:

— The incident wavelength λ_0 of the unperturbed laser beam radiation is very small, compared to the inner scale L_i of the turbulent inhomogeneities in the hot jet ($L_i = 1$ mm [24]).

— The whole path distance X traversed by the laser beam is very great, compared to the outer scale L_0 of the turbulent inhomogeneities ($L_0 = 10$ mm [19, 24]).

— The size of the first Fresnel zone $\sqrt{\lambda_0 X}$ is smaller than the inner scale L_i .

— The laser beam intensity fluctuations are neglected.

For the values of L_i and L_0 used here, we assume the experimental conditions we have applied in our previous papers [11, 19–21] about experiments for which a hot turbulent jet of air is considered as the

turbulent medium. These conditions are the same as those encountered in experiments carried out by Gagnaire and Tailland [24] for the same turbulent jet. So, we are allowed to use the measured values of the inner and outer scales they have obtained by means of the cold-wire anemometer technique.

Under the geometrical optics approximation, the random propagation of the laser beam may be approximated as a geometric walk process, that is, a walk process in which the laser beam undergoes only changes in direction such that the light beam can be regarded as a laser ray. Let $\varepsilon(M, t)$ be the random deflection angle of the laser beam defined from its unperturbed direction, at time t , for any point M of its trajectory in the medium. The purpose of this paper is to calculate the spatio-temporal correlation function $R_{\varepsilon\varepsilon} = \varepsilon(M_1, t_1)\varepsilon(M_2, t_2)$ of the laser beam deflection angles, corresponding to two points M_1 and M_2 , situated on the laser beam trajectory, at the instants t_1 and t_2 respectively ($t_1 < t_2$).

3. DETAILED APPROACH FOR THE CALCULATION OF THE CORRELATION OF DEFLECTION ANGLES OF THE LASER BEAM IN A TURBULENT MEDIUM

Since the geometrical optics approximation is assumed to be valid, let us write the ray equation:

$$\frac{d(n\boldsymbol{\tau})}{ds} = \nabla\mu \quad (1)$$

where ∇ denotes the gradient vector, $\boldsymbol{\tau}$ the unit vector tangent to the ray trajectory, s the arc length of the ray curve, and μ the fluctuation of the refractive index n around its mean value \bar{n} .

We assume that the ambient medium is at rest and that its refractive index n_0 remains constant. Under this condition, the laser beam direction $\boldsymbol{\tau}_0$ at the entry point O is assumed to be the unperturbed direction \mathbf{x} . Integrating Equation (1) along the laser beam trajectory, situated between the entry point O and a given point M defined in the medium, we obtain the following relation for any time t :

$$n\boldsymbol{\tau}(M, t) = \int_O^M \nabla\mu ds + n_0\boldsymbol{\tau}_0 \quad (2)$$

By using the vector product, this equation can be multiplied by \mathbf{x} and then gives:

$$n\boldsymbol{\tau}(M, t) \times \mathbf{x} = \int_O^M (\nabla\mu) \times \mathbf{x} ds \quad (3)$$

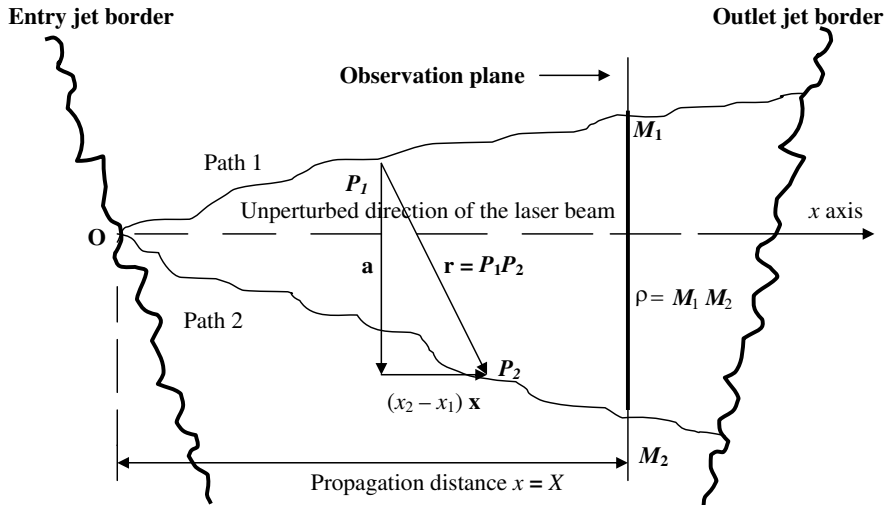


Figure 1. Scheme of two arbitrary paths of the laser beam used for determining the correlation functions of the light ray deflection angles: these functions are calculated for any observation plane perpendicular to the unperturbed laser beam direction.

We then introduce the unit vector \mathbf{u} perpendicular to the plane $(\mathbf{x}, \boldsymbol{\tau})$ and defined as: $\mathbf{u}(M, t) = (\boldsymbol{\tau} \times \mathbf{x}) / |\boldsymbol{\tau} \times \mathbf{x}|$. By taking into account the fact that the laser beam deflection angle ε is small ($\sin \varepsilon \approx \varepsilon$), we obtain the following relation:

$$n\varepsilon(M, t)\mathbf{u}(M, t) = \int_O^M (\nabla\mu) \times \mathbf{x} ds \tag{4}$$

which is equivalent to:

$$n\varepsilon(M, t)\mathbf{u}(M, t) = \int_O^M \left(-\frac{\partial\mu(P)}{\partial y} \mathbf{z} + \frac{\partial\mu(P)}{\partial z} \mathbf{y} \right) ds \tag{5}$$

where P is an arbitrary point situated on the laser beam trajectory, between the entry point O and given point M .

Let us consider two points $M_1 (X_1, Y_1, Z_1)$ and $M_2 (X_2, Y_2, Z_2)$ situated on two arbitrary trajectories of the laser beam and corresponding to two arc lengths s_1 and s_2 of the ray curve, as shown in Figure 1. By writing Equation (5) for M_1 and M_2 , we derive two

similar equations which can be multiplied; this gives:

$$\begin{aligned}
 & [(\bar{n} + \mu_1)\varepsilon_1(X_1, Y_1, Z_1, t_1)][(\bar{n} + \mu_2)\varepsilon_2(X_2, Y_2, Z_2, t_2)](\mathbf{u}_1 \cdot \mathbf{u}_2) \\
 &= \int_O^{M_1} \int_O^{M_2} \left(-\frac{\partial\mu_1(P_1, t_1)}{\partial y_1} \mathbf{z} + \frac{\partial\mu_1(P_1, t_1)}{\partial z_1} \mathbf{y} \right) \\
 & \quad \left(-\frac{\partial\mu_2(P_2, t_2)}{\partial y_2} \mathbf{z} + \frac{\partial\mu_2(P_2, t_2)}{\partial z_2} \mathbf{y} \right) ds_1 ds_2 \tag{6}
 \end{aligned}$$

where $P_1(x_1, y_1, z_1)$ and $P_2(x_2, y_2, z_2)$ are two arbitrary points situated on the trajectories (OM_1) and (OM_2) of the same laser beam, between O and M_1 , and between O and M_2 , respectively.

In the left-hand side of Equation (6), one has to neglect the quantities whose the orders of magnitude are very small compared to that of $(\bar{n})^2 \varepsilon_1(X_1, Y_1, Z_1, t_1)\varepsilon_2(X_2, Y_2, Z_2, t_2)$, that is, the quantities of third order $\bar{n}\mu_1\varepsilon_1\varepsilon_2$, $\bar{n}\mu_2\varepsilon_1\varepsilon_2$, and that of fourth order $\mu_1\mu_2\varepsilon_1\varepsilon_2$; in addition, the scalar product $\mathbf{u}_1 \cdot \mathbf{u}_2$ can be approximated to ± 1 because the smallness of the deflection angles of the laser beam along its whole path induces the smallness of the angle between the directions of the unit vectors \mathbf{u}_1 and \mathbf{u}_2 .

In the right hand side of Equation (6), we apply the following identity which is justified by the fact that the points P_1 and P_2 are independent, that is:

$$\begin{aligned}
 & \frac{\partial\mu_1(P_1)}{\partial y_1} \frac{\partial\mu_2(P_2)}{\partial y_2} = \frac{\partial}{\partial y_1} \left[\mu_1(P_1) \frac{\partial\mu_2(P_2)}{\partial y_2} \right] \\
 &= \frac{\partial}{\partial y_1} \left[\frac{\partial}{\partial y_2} (\mu_1(P_1)\mu_2(P_2)) \right] = \frac{\partial^2}{\partial y_1 \partial y_2} [\mu_1(P_1)\mu_2(P_2)] \tag{7}
 \end{aligned}$$

Let dx_1 and dx_2 be the projections of the curvilinear displacements ds_1 and ds_2 situated on the x axis. Since we have: $dx_1 = ds_1 \cos \alpha_1$ and $dx_2 = ds_2 \cos \alpha_2$ (α_1 and α_2 are the laser beam deflection angles at points P_1 and P_2 respectively), the quantities ds_1 and ds_2 are nearly equal to dx_1 and dx_2 respectively. This approximation holds because of the smallness of the laser beam deflection angles.

So, by averaging the resulting equation and by setting: $\tau = t_2 - t_1$, we obtain the following relation which represents the connection between the correlation function $R_{\varepsilon\varepsilon} = \overline{\varepsilon_1 \varepsilon_2}$ of the laser beam deflection angles, and the correlation function $R_{\mu\mu} = \overline{\mu_1 \mu_2}$ of the refractive index fluctuations, that is:

$$\begin{aligned}
 & R_{\varepsilon\varepsilon}(X_1, X_2, Y_1, Y_2, Z_1, Z_2, \tau) \\
 &= \pm \frac{1}{(\bar{n})^2} \int_0^{s_1} \int_0^{s_2} (\nabla \mathbf{a}_1 \cdot \nabla \mathbf{a}_2) R_{\mu\mu}(x_2 - x_1, y_2 - y_1, z_2 - z_1, \tau) dx_1 dx_2 \tag{8}
 \end{aligned}$$

In the above equation, $\nabla_{\mathbf{a}_1}$ and $\nabla_{\mathbf{a}_2}$ are the transversal gradients defined from the points P_1 and P_2 as follows:

$$\nabla_{\mathbf{a}_1} = \mathbf{y} \frac{\partial}{\partial y_1} + \mathbf{z} \frac{\partial}{\partial z_1}, \quad \nabla_{\mathbf{a}_2} = \mathbf{y} \frac{\partial}{\partial y_2} + \mathbf{z} \frac{\partial}{\partial z_2} \tag{9}$$

Let us introduce the transversal vector \mathbf{a} defined from the vectors $\mathbf{P}_1\mathbf{P}_2$ by the relation: $\mathbf{P}_1\mathbf{P}_2 = (x_2 - x_1)\mathbf{x} + \mathbf{a}$, that is: $\mathbf{a} = \mathbf{a}_2 - \mathbf{a}_1 = (y_2 - y_1)\mathbf{y} + (z_2 - z_1)\mathbf{z}$; this gives:

$$\nabla_{\mathbf{a}_1} \cdot \nabla_{\mathbf{a}_2} = -(\nabla_{\mathbf{a}})^2 \tag{10}$$

Hence, by applying the relation defined in Equation (10) and performing the integration defined in Equation (8), we obtain the following result:

$$R_{\varepsilon\varepsilon}(X_1, X_2, \boldsymbol{\rho}, \tau) = \frac{1}{(\bar{n})^2} \left| \int_0^{X_1} \int_0^{X_2} [(\nabla_{\mathbf{a}})^2 R_{\mu\mu}(x_2 - x_1, \mathbf{a}, \tau)]_{\mathbf{a}=\boldsymbol{\rho}} dx_1 dx_2 \right| \tag{11}$$

where $\boldsymbol{\rho} = \boldsymbol{\rho}_2 - \boldsymbol{\rho}_1 = (Y_2 - Y_1)\mathbf{y} + (Z_2 - Z_1)\mathbf{z}$ is the transversal vector defined from the vector $\mathbf{M}_1\mathbf{M}_2$ by the relation: $\mathbf{M}_1\mathbf{M}_2 = (X_2 - X_1)\mathbf{x} + \boldsymbol{\rho}$.

To simplify the result obtained in Equation (11), we use the fact that $R_{\mu\mu}$ depends on the variable $(x_2 - x_1)$, as it is shown in this equation. This suggests making a change of variables as follows:

$$x = x_2 - x_1 \tag{12a}$$

$$x_0 = (x_1 + x_2)/2 \tag{12b}$$

The integration defined in Equation (11) can then be transformed as a simple integration and gives the following result:

$$R_{\varepsilon\varepsilon}(X_1, X_2, \boldsymbol{\rho}, \tau) = \frac{(X_1 + X_2)}{2(\bar{n})^2} \left| \int_{-X_1}^{X_2} [(\nabla_{\mathbf{a}})^2 R_{\mu\mu}(x, \mathbf{a}, \tau)]_{\mathbf{a}=\boldsymbol{\rho}} dx \right| \tag{13}$$

Let us consider the practical case usually encountered in experimental applications, that is, the case for which the correlations of the laser beam deflection angles are observed at the detector plane, which is a transversal plane perpendicular to the unperturbed direction of the laser beam. The given points M_1 and M_2 used for evaluating the laser beam deflection angles are then situated on this observation plane supposed to be placed at a distance X from the entry point of the laser beam (See Figure 1). Hence, by setting $X_1 = X_2 = X$, and using the fact that correlations are even functions, we derive from Equation (13), the following result connecting the correlations $R_{\varepsilon\varepsilon}$ and $R_{\mu\mu}$:

$$R_{\varepsilon\varepsilon}(X, \boldsymbol{\rho}, \tau) = \frac{2X}{(\bar{n})^2} \left| \int_0^X [(\nabla_{\mathbf{a}})^2 R_{\mu\mu}(x, \mathbf{a}, \tau)]_{\mathbf{a}=\boldsymbol{\rho}} dx \right| \tag{14}$$

Since the parameter τ is defined as the time duration between the instants of measurements carried out at the points M_1 and M_2 , the value of this quantity should be arbitrarily imposed by the experimenter, as in conventional cases. However, for the spatio-temporal correlation functions $R_{\epsilon\epsilon}$ and $R_{\mu\mu}$ defined above, this value does not depend on the experimenter because it has the same order of magnitude as the time that light would take to travel between points M_1 and M_2 . So, the value of τ is very small and a series expansion in terms of powers of τ may then be done for the correlation function $R_{\mu\mu}$, that is:

$$\begin{aligned} \overline{\mu_1(P_1, t_1)\mu_2(P_2, t_1 + \tau)} &= \overline{\mu_1(P_1, t_1)\mu_2(P_2, t_1)} + \tau \overline{\mu_1(P_1, t_1) \frac{\partial \mu_2}{\partial t}(P_2, t_1)} \\ &+ \frac{\tau^2}{2} \overline{\mu_1(P_1, t_1) \frac{\partial^2 \mu_2}{\partial t^2}(P_2, t_1)} + \frac{\tau^3}{6} \overline{\mu_1(P_1, t_1) \frac{\partial^3 \mu_2}{\partial t^3}(P_2, t_1)} + \dots \end{aligned} \quad (15)$$

We need to determine the orders of magnitude of the quantities written in the right hand side of Equation (15). For this, we define t_i as the smallest timescale of the turbulence, that is, the Kolmogorov timescale. The order of magnitude of t_i is L_i/ν where ν is the Kolmogorov velocity scale and L_i the inner scale of the turbulence. By using the well-known Kolmogorov relation [25]:

$$\frac{\nu L_i}{\nu} = 1 \quad (16)$$

where ν denotes the kinematic viscosity ($\nu = 15.3 \times 10^{-6} \text{ m}^2/\text{s}$ for the jet considered), one can deduce that the order of magnitude of t_i is $L_i^2/\nu = 0.065 \text{ s}$. Since the order of magnitude of τ is L_0/c where L_0 represents the outer scale of the turbulence and c the velocity of light ($L_0/c \approx 0.033 \times 10^{-10} \text{ s}$), we derive that the orders of magnitude of the quantities mentioned in the right hand side of Equation (15) are respectively: $\overline{\mu^2}$, $\left(\frac{L_0 c^{-1}}{t_i}\right) \overline{\mu^2}$, $\left(\frac{L_0 c^{-1}}{t_i}\right)^2 \overline{\mu^2}$, $\left(\frac{L_0 c^{-1}}{t_i}\right)^3 \overline{\mu^2}$. So, the second, third, and the fourth quantities in the right hand side of Equation (15) are very small compared to $\overline{\mu_1(P_1, t_1)\mu_2(P_2, t_1)}$. We then find that the following approximation may be applied:

$$\overline{\mu_1(P_1, t_1)\mu_2(P_2, t_1 + \tau)} \approx \overline{\mu_1(P_1, t_1)\mu_2(P_2, t_1)} \quad (17)$$

This leads to conclusion that the spatio-temporal correlations of the laser beam deflection angles in a turbulent jet can be regarded as spatial correlations for all experimental processes in which the time duration between the measurements of the deflection angles at the correlation points is very small compared to the Kolmogorov timescale. In the rest of this work, we assume that this condition is satisfied.

Therefore, we are allowed to omit the parameter τ among the variables on which depend the correlation functions $R_{\mu\mu}$ and $R_{\varepsilon\varepsilon}$.

As suggested by Tatarskii [1], we assume that the hypothesis of local isotropy and homogeneity is valid, that is: $R_{\varepsilon\varepsilon}(X, \boldsymbol{\rho}) = R_{\varepsilon\varepsilon}(X, \rho)$ and $R_{\mu\mu}(\mathbf{r}) = R_{\mu\mu}(r)$, with $\rho = |\boldsymbol{\rho}|$ and $r = |\mathbf{r}| = \sqrt{x^2 + \rho^2}$. We then obtain the following relation:

$$R_{\varepsilon\varepsilon}(X, \rho) = \frac{2X}{(\bar{n})^2} \left| \int_0^X \left[\frac{\rho^2}{r^2} \frac{d^2 R_{\mu\mu}(r)}{dr^2} + \left(\frac{2}{r} - \frac{\rho^2}{r^3} \right) \frac{dR_{\mu\mu}(r)}{dr} \right] dx \right| \quad (18)$$

The relation we have obtained in Equation (18) enables to calculate the correlations of the laser beam deflection angles if the correlations of the refractive index fluctuations are known.

4. COMPLETED FORMULAS BY APPLYING THE MODELS OF TURBULENCE

To apply the correlation functions $R_{\mu\mu}(r)$ of the refractive index fluctuations in Equation (18), we need to know the spectrum of turbulence in the heated medium, that is, the function $\phi_\mu(K)$ which depends on the wave number K and is connected to $R_{\mu\mu}(r)$ by the well-known relation [1]:

$$R_{\mu\mu}(r) = 4\pi \int_0^\infty K \phi_\mu(K) \left(\frac{\sin(Kr)}{r} \right) dK \quad (19)$$

By using Equation (19), we obtain for any position X of the observation plane, the final expression of $R_{\varepsilon\varepsilon}(X, \rho)$:

$$R_{\varepsilon\varepsilon}(X, \rho) = \frac{8\pi}{(\bar{n})^2} X \left| \int_0^X \left(\int_0^\infty K \phi_\mu(K) f(K, x, \rho) dK \right) dx \right| \quad (20)$$

where the function $f(K, x, \rho)$ is defined as:

$$f(K, x, \rho) = \left(\frac{K^2 \rho^2 + 2}{r^3} - \frac{3\rho^2}{r^5} \right) \sin(Kr) + \left(\frac{3K\rho^2}{r^4} - \frac{2K}{r^2} \right) \cos(Kr) \quad (21)$$

An equivalent equation for the definition of $f(K, x, \rho)$ can be derived by using the spherical Bessel functions of first kind j_m [26]. This gives:

$$f(K, x, \rho) = \frac{2K^2}{r} j_1(Kr) - \frac{K^3 \rho^2}{r^2} j_2(Kr) \quad (22)$$

To calculate $R_{\varepsilon\varepsilon}(X, \rho)$ from Equation (20), we need for practical reasons, to introduce the following non dimensional variables: $\sigma = K/K_m$, $\sigma_0 = K_0/K_m$, $\xi = K_m x$, $\eta = K_m \rho$, and $p = K_m r = \sqrt{\xi^2 + \eta^2}$.

The wave numbers $K_0 = 1/L_0$ and $K_m = 5.92/L_i$ are the two limits of the inertial zone of turbulence, L_0 and L_i being the outer and inner scales of the turbulence respectively.

Moreover, for usual experimental conditions, the observation plane is placed at a distance X very large compared to the correlation distance of the refractive index fluctuations. This enables the renewal of the optical turbulence for a great number of times before reaching the observation plane, in order to obtain reliable measurements evaluated at this plane. Hence, the upper limit of the integration defined in Equation (20) can be extended to infinity.

From Equation (20), we find that the correlation function $R_{\epsilon\epsilon}$ is given by the following relation using the above non dimensional variables:

$$R_{\epsilon\epsilon}(X, \eta) = \frac{8\pi}{(\bar{n})^2} K_m^4 X \left| \int_0^\infty \left(\int_0^\infty \sigma \phi_\mu(\sigma) \left(\left(\frac{\sigma^2 \eta^2 + 2}{p^3} \right) \sin(p\sigma) + \left(\frac{3\sigma \eta^2}{p^4} - \frac{2\sigma}{p^2} \right) \cos(p\sigma) \right) d\sigma \right) d\xi \right| \quad (23)$$

where $\phi_\mu(\sigma)$ is the dimensionless expression of $\phi_\mu(K)$.

4.1. The Von Karman Model

To model the spectrum of turbulence for the refractive index fluctuations, we assume the classical hypothesis of the Kolmogorov spectrum [25] which reveals a $-11/3$ power law for the inertial zone of turbulence, but does not give satisfactory results for small wave numbers. To define the turbulence spectrum valid for all wave numbers, one usually needs to complete the Kolmogorov spectrum for small values of the wave number. This enables to obtain the more completed model called the Von Karman spectrum, and defined by the following relation [3, 15]:

$$\phi_\mu(K) = 0.033 C_\mu^2 (K^2 + K_0^2)^{-11/6} \exp\left(-\frac{K^2}{K_m^2}\right) \quad (24a)$$

which is equivalent to the non-dimensional form:

$$\phi_\mu(\sigma) = 0.033 C_\mu^2 K_m^{-11/3} (\sigma^2 + \sigma_0^2)^{-11/6} \exp(-\sigma^2) \quad (24b)$$

In Equations (24a) and (24b), C_μ^2 is the structure coefficient of the refractive index fluctuations in the turbulent medium.

By using Equation (24b), the result obtained in Equation (23) becomes:

$$R_{\epsilon\epsilon}(X, \eta) = \frac{0.264\pi}{(\bar{n})^2} C_\mu^2 K_m^{1/3} X \left| \int_0^\infty \phi_1(\xi, \eta) d\xi \right| \quad (25)$$

where the function $\phi_1(\xi, \eta)$ is defined as follows:

$$\phi_1(\xi, \eta) = \int_0^\infty \sigma (\sigma^2 + \sigma_0^2)^{-11/6} \exp(-\sigma^2) \left[\left(\frac{\sigma^2 \eta^2 + 2}{p^3} - \frac{3\eta^2}{p^5} \right) \sin(p\sigma) + \left(\frac{3\sigma \eta^2}{p^4} - \frac{2\sigma}{p^2} \right) \cos(p\sigma) \right] d\sigma \quad (26)$$

4.2. The Tatarskii Model

This model is less realistic than the model of Von Karman because it does not take into account the existence of the outer scale of turbulence L_0 , that is, the lower limit K_0 of the inertial zone of the turbulence spectrum. The Tatarskii model is deduced from the Von Karman model by setting: $K_0 = 0$. So, it is defined as [1]:

$$\phi_\mu(K) = 0.033 C_\mu^2 K^{-11/3} \exp\left(-\frac{K^2}{K_m^2}\right) \quad (27a)$$

that is:

$$\phi_\mu(\sigma) = 0.033 C_\mu^2 K_m^{-11/3} \sigma^{-11/3} \exp(-\sigma^2) \quad (27b)$$

By using Equation (27b), Equation (23) gives:

$$R_{\varepsilon\varepsilon}(X, \eta) = \frac{0.264\pi}{(\bar{n})^2} C_\mu^2 K_m^{1/3} X \left| \int_0^\infty \phi_2(\xi, \eta) d\xi \right| \quad (28)$$

where the function $\phi_2(\xi, \eta)$ is defined as:

$$\phi_2(\xi, \eta) = \int_0^\infty \sigma^{-8/3} \exp(-\sigma^2) \left[\left(\frac{\sigma^2 \eta^2 + 2}{p^3} - \frac{3\eta^2}{p^5} \right) \sin(p\sigma) + \left(\frac{3\sigma \eta^2}{p^4} - \frac{2\sigma}{p^2} \right) \cos(p\sigma) \right] d\sigma \quad (29)$$

5. NUMERICAL RESULTS: CALCULATION OF THE STRUCTURE COEFFICIENT OF REFRACTIVE INDEX FLUCTUATIONS AND DEDUCTION OF CORRELATIONS OF THE LASER BEAM DEFLECTION ANGLES

The method which enables to determine the structure coefficient of the refractive index fluctuations for the hot turbulent jet uses the diffusion coefficient. Introduced by Chernov [2], this coefficient is usually noted by D_μ . It was calculated in our previous works [11, 19–21] and is connected to the variance of the laser beam deflection angle, according to the Chernov law [2]:

$$\overline{\varepsilon^2} = \frac{4}{(\bar{n})^2} D_\mu X \quad (30)$$

where D_μ is defined as [2, 11, 19–21]:

$$D_\mu = -\frac{1}{2} \int_0^\infty \nabla^2 R_{\mu\mu}(r, 0, 0) dr = -\int_0^\infty \frac{1}{r} \left(\frac{dR_{\mu\mu}(r, 0, 0)}{dr} \right) dr \quad (31)$$

It should be explicitly stated that:

$$\overline{\varepsilon^2} = R_{\varepsilon\varepsilon}(X, \eta = 0) = \frac{0.264\pi}{(\bar{n})^2} C_\mu^2 K_m^{1/3} X \left| \int_0^\infty \phi(\xi, 0) d\xi \right| \quad (32)$$

where the function ϕ is equal to ϕ_1 or ϕ_2 for the Karman and Tatarskii models, respectively.

The result we have obtained in Equation (32) shows that the variance of the laser beam deflection angles is proportional to the propagation distance X ; this agrees with the Chernov law. In addition, we deduce from Equations (30) and (32) that the structure coefficient C_μ^2 is given by the following relation:

$$C_\mu^2 = \frac{D_\mu}{0.066\pi K_m^{1/3} \left| \int_0^\infty \phi(\xi, 0) d\xi \right|} \quad (33)$$

For numerical calculations, all integrations are performed by means of the Simpson algorithms [27], and for the results thus obtained, the convergence requirements are ensured. The integration interval along the ξ axis, whose length is represented by δ , is then discretized in $(N+1)$ small intervals of same length $\Delta\xi$ such that $\Delta\xi/\delta = 10^{-4}$. So, the well-known [27] condition of convergence $\Delta\xi/\delta \leq 10^{-2}$ is satisfied. Since the upper limit of the Von Karman spectrum corresponds to the value $\sigma = 1$, the integrations extended to infinity and defined in Equations (26) and (29) can be computed in the interval $[0, \sigma_m]$ such that $\sigma_m \gg 1$. This interval is then discretized in $(M+1)$ small intervals of same length $\Delta\sigma$ such that $\Delta\sigma/\sigma_m = 10^{-4}$.

In all numerical processes, we need the quantity $\phi_0 = \phi(\xi = 0, \eta = 0)$; but this value cannot be directly calculated because the function $\phi(\xi, \eta)$ presents a singularity for $\xi = \eta = 0$. For this, we apply a Taylor series expansion of ϕ in the neighbourhood of the point $\xi = 0$. After integration, we find the following result:

— for the Von Karman model

$$\begin{aligned} \phi_0 &= \phi_1(\xi = 0, \eta = 0) \\ &= \frac{2}{3} \int_0^\infty \sigma^4 (\sigma^2 + \sigma_0^2)^{-11/6} \exp(-\sigma^2) d\sigma = 0.4440 \end{aligned} \quad (34)$$

— for the Tatarskii model.

$$\phi_0 = \phi_2(\xi = 0, \eta = 0) = \frac{2}{3} \int_0^\infty \sigma^{1/3} \exp(-\sigma^2) d\sigma = 0.4471 \quad (35)$$

In Table 1, we present the values of the quantities $A_1 = \int_0^{K_m X} \phi_1(\xi, 0)d\xi$ and $A_2 = \int_0^{K_m X} \phi_2(\xi, 0)d\xi$ as functions of X , and this is a demonstration that A_1 and A_2 converge as X increases. These quantities are needed in Equations (25) and (28) for the derivation of the correlation curves. From the values presented in Table 1, the convergence curves of the quantities A_1 and A_2 are plotted in Figure 2. These curves show that for $X \geq 50$ mm, A_1 converges to 2.94 and A_2 converges to 3.42.

To obtain numerical results by applying Equations (25), (28)

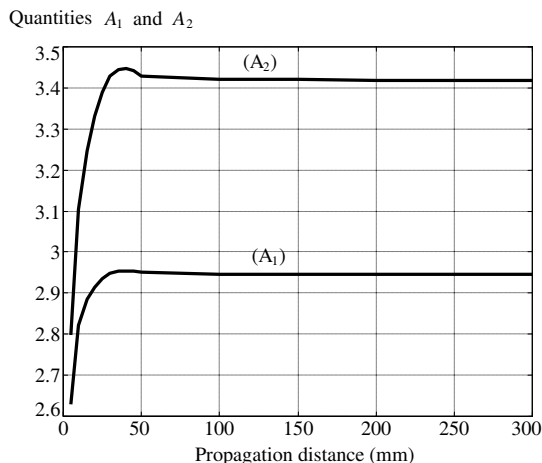


Figure 2. Convergence curves of the quantities $A_1(X) = \int_0^{K_m X} \phi_1(\xi, 0)d\xi$ and $A_2(X) = \int_0^{K_m X} \phi_2(\xi, 0)d\xi$ as X increases. $A_1(\infty) = 2.94$ and $A_2(\infty) = 3.42$ for the Karman and Tatarskii models respectively.

Table 1. Values of the quantities $A_1(X) = \int_0^{K_m X} \phi_1(\xi, 0)d\xi$ and $A_2(X) = \int_0^{K_m X} \phi_2(\xi, 0)d\xi$: Convergence of A_1 and A_2 as X increases.

X (mm)	5	10	20	30	40	50
A_1	2.63	2.82	2.91	2.94	2.95	2.94
A_2	2.79	3.10	3.33	3.42	3.44	3.42

X (mm)	100	150	200	250	300
A_1	2.94	2.94	2.94	2.94	2.94
A_2	3.42	3.42	3.42	3.42	3.42

and (33), one needs the value of the diffusion coefficient D_μ of the turbulent medium, since the limits of the inertial zone of turbulence $K_0 = 1/L_0$ and $K_m = 5.92/L_i$ are known. For this, we use the best result ($D_\mu = 2.18 \times 10^{-9} \text{ m}^{-1}$) we have found [11], among the values calculated in our previous works. Hence, by using the computed values of the quantities A_1 and A_2 , we have obtained the following result from Equation (33): $C_\mu^2 = 1.97 \times 10^{-10} \text{ m}^{-2/3}$ and $C_\mu^2 = 1.70 \times 10^{-10} \text{ m}^{-2/3}$, for the Karman and Tatarskii models, respectively.

The computed values of C_μ^2 are then used in Equations (25) and (28) for evaluating the correlation functions $R_{\varepsilon\varepsilon}$ of deflection angles of the laser beam, by setting $\bar{n} = 1$ for the air of the jet. The results we have thus obtained are plotted in Figure 3 for the Karman model and, in Figure 4 for the Tatarskii model, for four values of the propagation distance: $X = 50 \text{ mm}$, 100 mm , 200 mm , and 300 mm . To compare the results obtained from the two models, we need to plot in the same figure the correlation function of deflection angles of the laser beam, computed from the two models, for a given propagation distance. This is done in Figure 5 for $X = 200 \text{ mm}$. This figure demonstrates that the values of the correlation function of the laser beam deflection angles obtained from the Tatarskii model ($R_{\varepsilon\varepsilon}^T(X, \eta)$) are greater than those given by the Karman model ($R_{\varepsilon\varepsilon}^K(X, \eta)$). To evaluate the difference

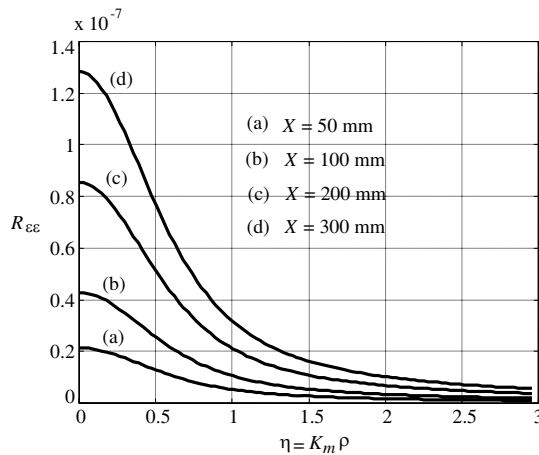


Figure 3. Correlation functions of the laser beam deflection angles in the turbulent jet of air (Karman model) as function of $\eta = K_m \rho$, for four values of the propagation distance: (a) $X = 50 \text{ mm}$; (b) $X = 100 \text{ mm}$; (c) $X = 200 \text{ mm}$; (d) $X = 300 \text{ mm}$.

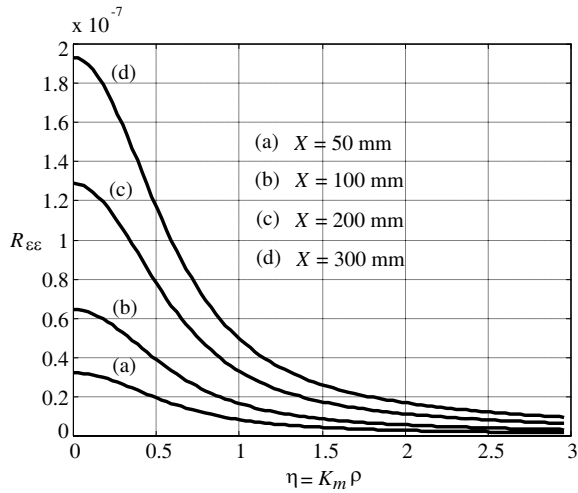


Figure 4. Correlation functions of the laser beam deflection angles in the turbulent jet of air (Tatarskii model) as function of $\eta = K_m \rho$, for four values of the propagation distance: (a) $X = 50$ mm; (b) $X = 100$ mm; (c) $X = 200$ mm; (d) $X = 300$ mm.

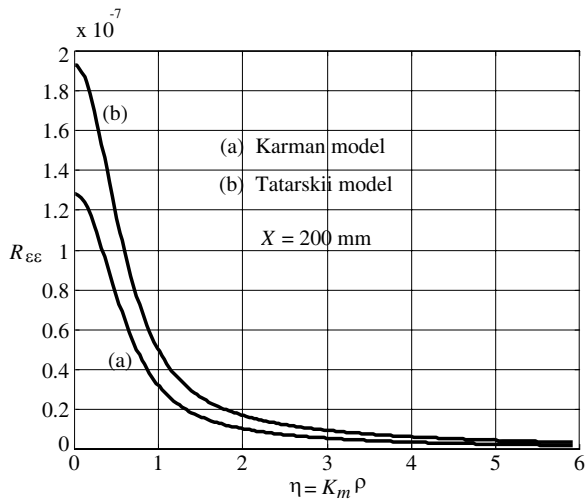


Figure 5. Comparison between the Karman and Tatarskii models: The correlation function of deflection angles of the laser beam for $X = 200$ mm.

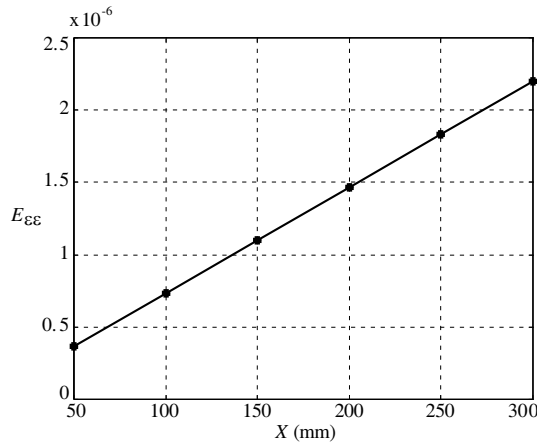


Figure 6. The difference between the correlation function of the laser beam deflection angles derived from the Karman and Tatarskii models plotted as function of the propagation distance.

between both models, we consider the quantity $E_{\epsilon\epsilon}$ defined as:

$$E_{\epsilon\epsilon}(X) = \int_0^{\infty} (R_{\epsilon\epsilon}^T(X, \eta) - R_{\epsilon\epsilon}^K(X, \eta)) d\eta \quad (36)$$

Figure 6 shows that $E_{\epsilon\epsilon}$ increases linearly as function of the propagation distance. This was expected because the correlations obtained from the models are linear functions of the propagation distance.

6. VALIDATION PROCESS OF THE COMPUTED RESULTS: EXPERIMENTS FOR THE MEASUREMENT OF STRUCTURE COEFFICIENT OF THE REFRACTIVE INDEX FLUCTUATIONS IN HOT TURBULENT JET

In the view of validating the results we have obtained, we carry out experiments in which we measure the structure coefficient C_{μ}^2 of the refractive index for the jet considered, and compare the experimental result to the theoretical values achieved in Section 5.

To measure C_{μ}^2 , one might apply the scintillometer technique. It is a well-known powerful method that many scientists [28, 29] are making increasing use for the measurement of C_{μ}^2 in a turbulent atmosphere. This laser-based technique uses a photoelectric cell which enables to find C_{μ}^2 from the measurement of the intensity fluctuations of a laser beam transecting the turbulent medium, and the results are all the

more accurate as the intensity fluctuations of the laser beam are strong. For this, laser beams having large diameters (15 cm–30 cm) are usually used and large distances of propagation (250 m–8.5 km) are applied, such that the laser beams undergo important diffraction effects. Since the geometrical optics approximation used in this work is not valid for the scintillometer technique, we cannot exploit this technique for the measurement of the structure coefficient C_{μ}^2 .

The technique that we have applied is one in which the measurement of C_{μ}^2 is performed from the luminous trace produced by a laser beam on the plane of a position photocell, after having traversed the jet. More precisely, the experimental values of C_{μ}^2 are deduced from the measurement of the probabilities of the positions of the laser beam impact on the photocell.

The experimental setup already used in previous works [19–21] is shown schematically in Figure 7. The laser beam (wavelength $\lambda_0 = 6328 \text{ \AA}$, initial diameter = 0.8 mm) created from a 1 mW He-Ne laser, is passed through a hot turbulent jet of air issued from a rectangular nozzle of a wind tunnel. The nozzle aperture has the same dimensions (200 mm \times 47 mm) as in [11, 24]. Assuming Gagnaire's experimental conditions [24], the unperturbed direction of the laser beam is perpendicular to the jet exhaust, and is placed in the xy plane ($z = 0$), at the distance $y = d$ from the plane of the nozzle aperture. Outside the jet, at a distance D from the outlet jet border, the photocell is placed perpendicularly to the unperturbed direction of the laser beam. The photocell transmits two electrical signals whose amplitudes are proportional to the coordinates of the beam impact. In the absence of the jet, the ambient medium is at rest; the laser beam trajectory remains nearly rectilinear. In that case, the two voltages derived from the photocell are adjusted to be equal to zero; the corresponding beam impact which we have called "initial impact" is taken to be the origin of the photocell plane, that is, the point from which the transverse displacement of the laser beam impact is measured. With the aim to obtain experimental results for various values of the jet width traversed by the laser beam, the distance d varies. For this, the mirror shown in Figure 7 moves parallel to itself and for each position of the mirror, the position of the photocell is adjusted such that it contains the same initial impact.

During propagation, the laser beam remains thin, and the conditions which justify the applicability of the geometrical optics approximation described in Section 2, are rigorously satisfied.

The measurement method for the probabilities $P(y, z)$ of the positions (y, z) of the laser beam impact on the photocell plane has already been detailed in previous papers [19–21]. As explained in [19–

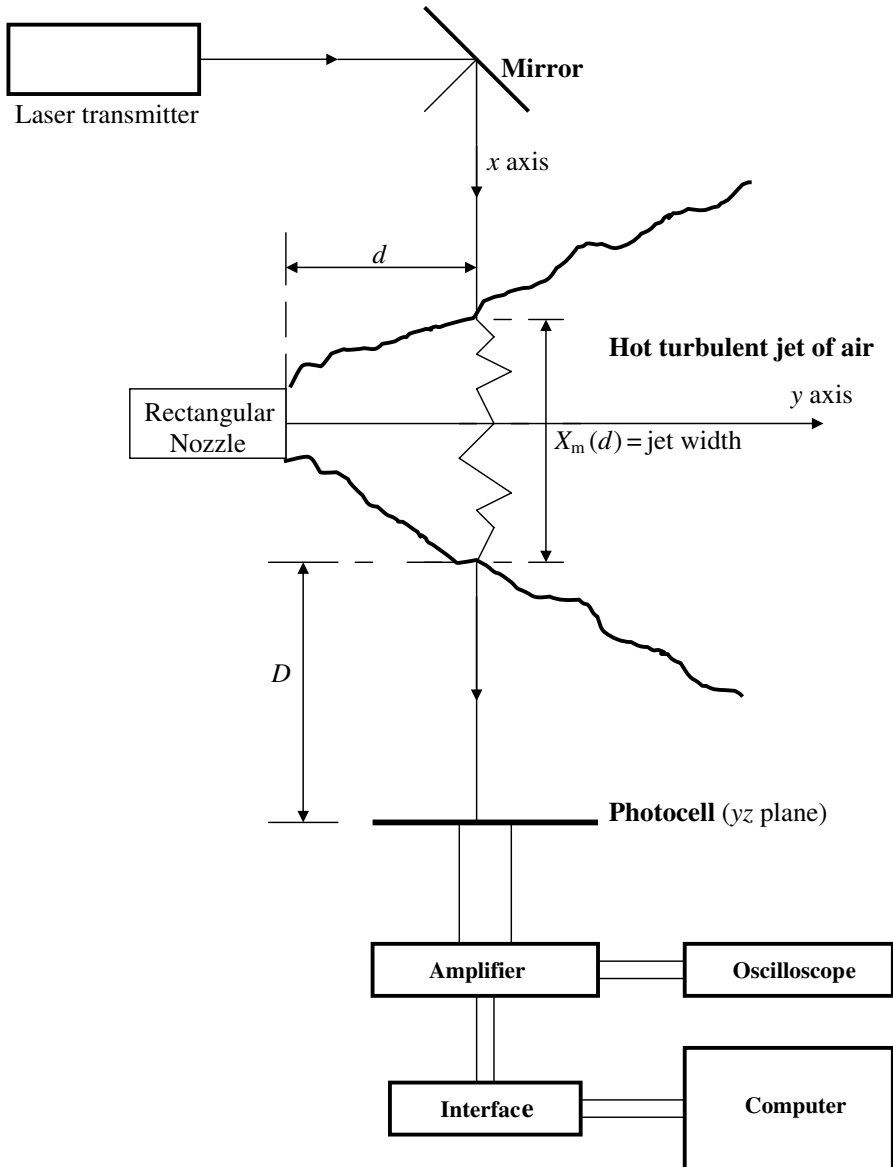


Figure 7. Experimental setup for the measurement of the probabilities of the positions of the laser beam impact on the photocell plane.

21], the photocell plane is cross-ruled in 1600 small squares of the same size c , defined as follows:

$$Y(j) = Y_0 + j \cdot c, \quad j = 0, 1, \dots, j_{\max} \quad (j_{\max} = 40) \quad (37a)$$

$$Z(k) = Z_0 + k \cdot c, \quad k = 0, 1, \dots, k_{\max} \quad (k_{\max} = 40) \quad (37b)$$

$$c = 0.01 \text{ cm} \quad (37c)$$

$$Y_0 = Z_0 = -0.20 \text{ cm} \quad (37d)$$

The quantity $P(y, z)$ is the probability for the laser beam impact centre (y, z) to be situated within the square $([Y(j), Y(j+1)]; [Z(k), Z(k+1)])$. The lower limits (Y_0, Z_0) and the upper limits $(Y(j_{\max}), Z(k_{\max}))$ are defined such that the entire measuring square contains a set of 80×80 small squares of same size $c = 0.01$ cm. After having eliminated the points for which probabilities are equal to zero, this initial square is reduced to the minimal square able to contain the luminous trace produced by the laser beam on the photocell. The final measuring domain in which statistical investigations are carried out is then obtained as a square containing 40×40 small squares of size c , and defined by: $Y_0 \leq y \leq Y(j_{\max})$ and $Z_0 \leq z \leq Z(k_{\max})$ with $Y_0 = Z_0 = -0.20$ cm and $Y(j_{\max}) = Z(k_{\max}) = 0.20$ cm. So, the above measuring process which does not reduce the accuracy of measurements enables to deal with an optimal number of useful data for statistical investigations.

The diameter (0.90 mm) of the laser beam footprint represents 22.5% of the size of the final measuring square. The surface occupied by this footprint (0.63 mm^2) represents 4% of the surface of the final measuring square.

By using a more powerful device, we have obtained more accurate measurements: the interface enables to store $2 \times (2^8 \times 2^8) = 131072$ impacts in approximately 20 seconds; this gives a time duration $\tau = 1.52 \times 10^{-1}$ ms between two successive stored impacts, which is smaller compared to the Kolmogorov timescale $t_i = 0.065$ s. So, we can apply the approximation defined in Equation (17) which allows considering the spatio-temporal correlations $R_{\varepsilon\varepsilon}$ as spatial functions.

The values we have obtained for the probabilities $P(Y, Z)$ are plotted in Figures 8(a), 8(b), and 8(c). In Figures 9(a), 9(b), and 9(c) the corresponding luminous trace produced by the laser beam on the photocell are presented. The marginal probabilities deduced from the probabilities $P(Y, Z)$ are shown in Figures 10(a), 10(b), and 10(c) for the Z coordinate, and in Figures 11(a), 11(b), and 11(c) for the Y coordinate. The behaviour of these marginal probabilities is studied as function of the jet width X_m and the curves obtained are presented in Figures 12 and 13. The figures of the probabilities show clearly that the central region of the plane of the photocell coincides with

the region surrounding the initial impact of the laser beam. In this area defined as the luminous trace produced by the laser beam on the photocell (Figures 9(a), 9(b), 9(c)), one observes that the values of the probabilities of the positions of the laser beam impact are not equal to zero. In Figures 9(a), 9(b), 9(c), 12 and 13, it is shown that, as the propagation distance traversed by the laser beam increases, the maximum of the probabilities decreases whereas the surface of the luminous trace increases. This phenomenon of diffusion of the laser beam direction in the turbulent jet is consistent with the fact that the sum of the probabilities must remain equal to 1, even if the propagation distance varies.

To deduce the structure coefficient C_μ^2 from the measurement of

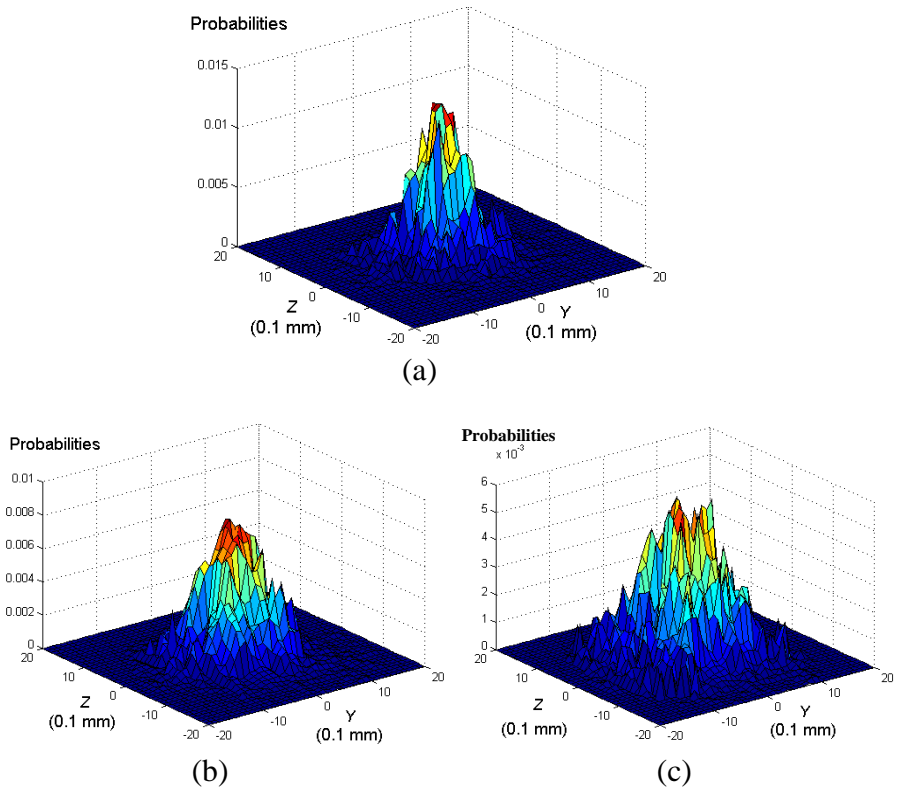


Figure 8. Probabilities of the laser beam impact positions on the plane of the photocell: (a) $X_m = 200$ mm; (b) $X_m = 300$ mm; (c) $X_m = 400$ mm.

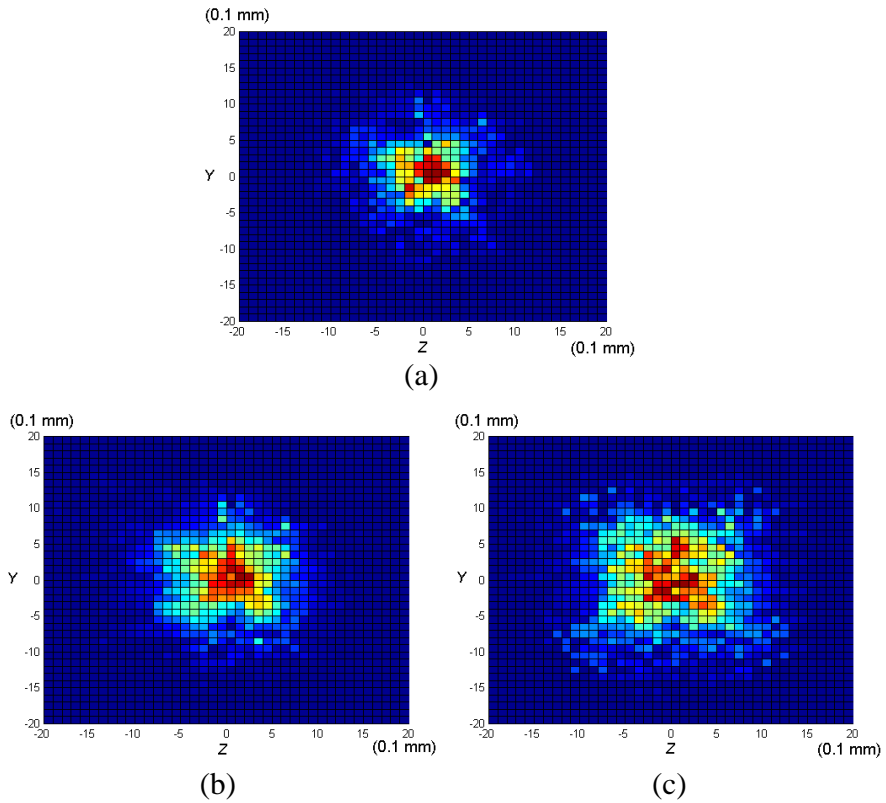


Figure 9. Luminous trace of the laser beam on the plane of the photocell: (a) $X_m = 200$ mm; (b) $X_m = 300$ mm; (c) $X_m = 400$ mm.

the probabilities, we exploit the formula which gives the variance of the transverse displacement ρ of the laser beam in terms of the structure coefficient of the refractive index fluctuations, the inner scale L_i of the turbulence, and the propagation distance X , that is [12, 16]:

$$\overline{\rho^2} = 2.2C_\mu^2 X^3 L_i^{-1/3} \tag{38}$$

The deflection angle of the laser beam being small, we can assume [19] that the polar and azimuthal angles (ϕ, θ) , which characterize the laser beam direction at any point of its trajectory in the turbulent jet, are nearly equal to the corresponding angles of the position vector at the same point. Also, if (y_m, z_m) are the coordinates of the laser beam impact on the outlet border of the jet corresponding

to the width ($x = X_m$) of the jet, it can be shown that:

$$y_m = X_m \tan \phi \quad (39a)$$

$$z_m = X_m \cot \theta / \cos \phi \quad (39b)$$

It is obvious that the angles (ϕ, θ) are random functions which depend on the propagation distance of the laser beam. But all possible values of each angle belong to a set which remains unchanged because we assume [19, 21] that it contains the same elements as the propagation distance varies. In addition, we assume that the values of these elements depend only on the laser beam impact position on the photocell. Hence, the propagation of the laser beam being rectilinear

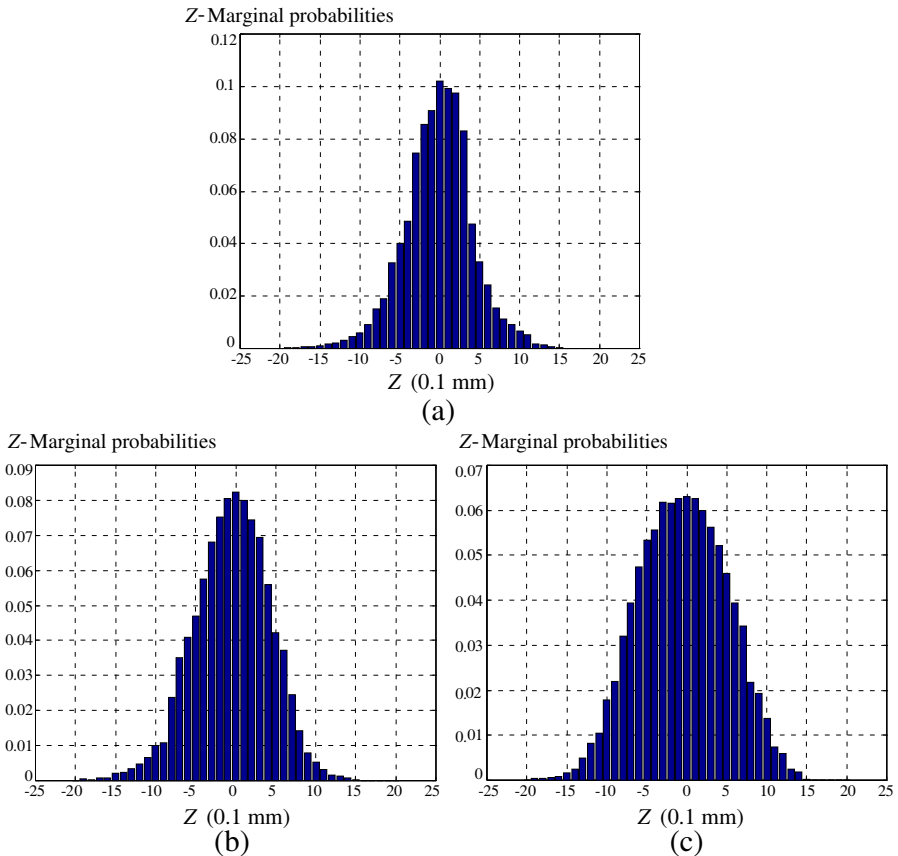


Figure 10. Marginal probabilities of the Z coordinate of the laser beam impact on the photocell: (a) $X_m = 200$ mm; (b) $X_m = 300$ mm; (c) $X_m = 400$ mm.

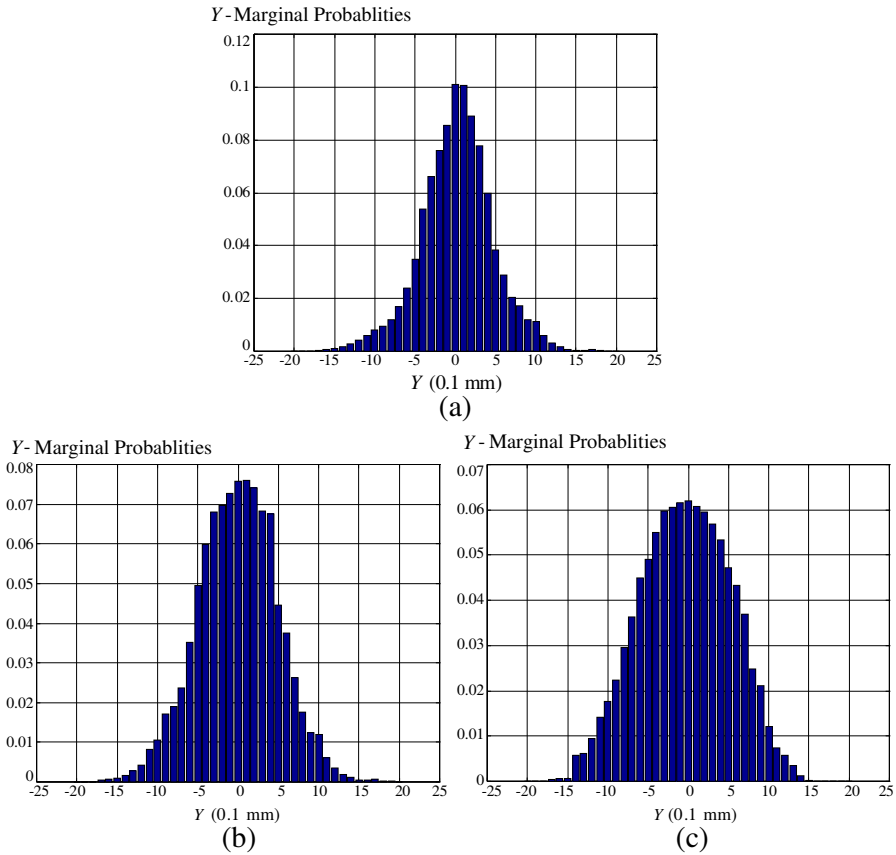


Figure 11. Marginal probabilities of the Y coordinate of the laser beam impact on the photocell: (a) $X_m = 200$ mm; (b) $X_m = 300$ mm; (c) $X_m = 400$ mm.

from the outlet jet border to the photocell, it can be demonstrated that the transverse displacement ρ_m of the laser beam at the outlet of the jet is connected to its transverse displacement ρ_{cell} measured on the photocell plane, by the following relation:

$$\rho_m = \left(\frac{X_m}{X_m + D} \right) \rho_{cell} \tag{40}$$

Applying Equation (38), the above relation gives:

$$\left(\frac{X_m}{X_m + D} \right)^2 \frac{1}{\rho_{cell}^2} = 2.2 C_\mu^2 X_m^3 L_i^{-1/3} \tag{41a}$$

that is:

$$\left(\frac{1}{X_m + D}\right)^2 \overline{\rho_{\text{cell}}^2} = \left(2.2C_\mu^2 L_i^{-1/3}\right) X_m \tag{41b}$$

Equation (41b) shows that the structure coefficient C_μ^2 of the refractive index fluctuations can be found if the quantity $\overline{\rho_{\text{cell}}^2}$ is known. Let us

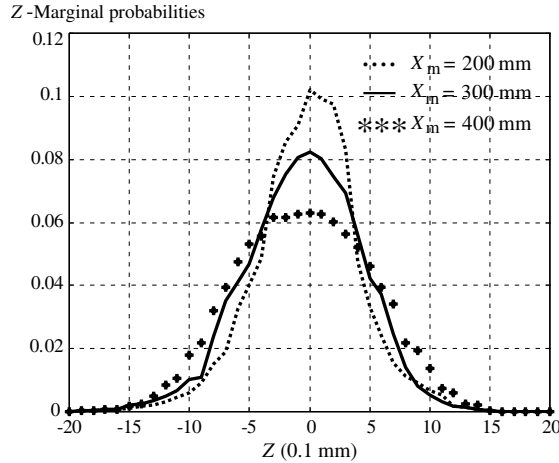


Figure 12. Comparison between the Z marginal probabilities as the jet width varies.

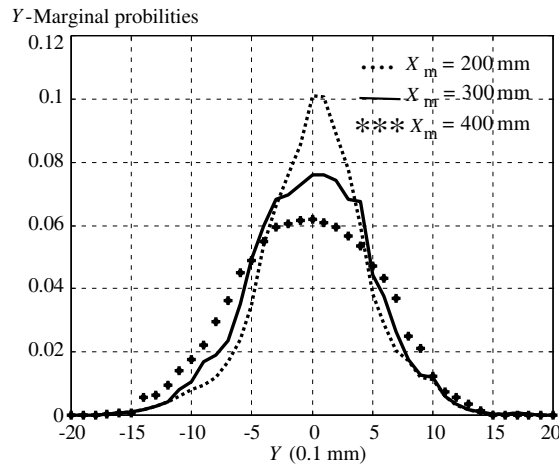


Figure 13. Comparison between the Y marginal probabilities as the jet width varies.

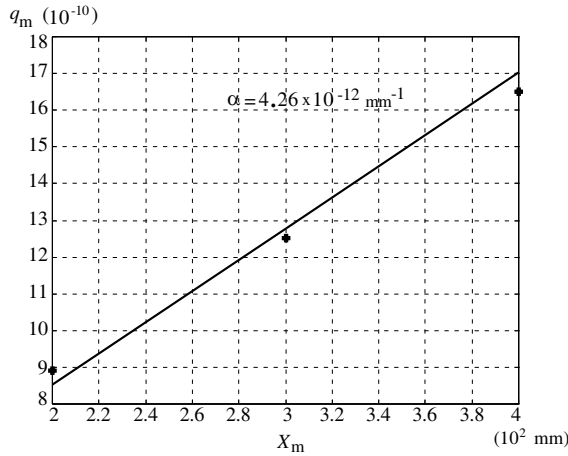


Figure 14. Quantity q_m as function of the jet width X_m : Measurement of the slope α and deduction of the structure coefficient C_μ^2 of the hot turbulent jet.

define the quantity q_m as follows:

$$q_m = \left(\frac{1}{X_m + D} \right)^2 \overline{\rho_{\text{cell}}^2} \tag{42}$$

Equation (41b) demonstrates that the values of q_m vary as a linear function of the width X_m of the jet, according to a straight line with the slope α given by:

$$\alpha = \left(2.2C_\mu^2 L_i^{-1/3} \right) \tag{43}$$

To measure α , we need the marginal probabilities $P_{\text{mar}}(Y)$ and $P_{\text{mar}}(Z)$ of the coordinates Y and Z of the laser beam impact position on the photocell. These probabilities are extracted from the measured probabilities $P(Y, Z)$ and are plotted in Figures 10(a), 10(b), 10(c), and 11(a), 11(b), 11(c). The quantities q_m are measured from the variance of the transverse displacement $\overline{\rho_{\text{cell}}^2}$ of the laser beam impact, where $\overline{\rho_{\text{cell}}^2}$ is given by :

$$\overline{\rho_{\text{cell}}^2} = \int Y^2 P_{\text{mar}}(Y) dY + \int Z^2 P_{\text{mar}}(Z) dZ \tag{44}$$

In Table 2, we present the values of q_m obtained for different entry points of the laser beam corresponding to three values of the jet width X_m . The curve which represents the behaviour of q_m as function of X_m is shown in Figure 14. The slope α derived from this figure is:

Table 2. Experimental values for the derivation of the quantity q_m as a function of the jet width X_m .

d (mm)	D (mm)	X_m (mm)	$\overline{\rho_{\text{cell}}^2}$ (10^{-3} mm ²)	q_m (10^{-10})
121	600	200	0.56	8.90
200	650	300	1.12	12.50
280	695	400	1.97	16.50

Table 3. Comparison between the theoretical predictions and the experimental measurement of the structure coefficient of the turbulent jet.

Methods	Tatarskii model	Karman model	Experiments
Values of C_μ^2 (10^{-10} m ^{-2/3})	1.70	1.97	1.93

$\alpha = 4.26 \times 10^{-12}$ mm⁻¹. Hence, the value of the structure coefficient C_μ^2 can be computed by using Equation (43). This gives:

$$C_\mu^2 = 1.93 \times 10^{-10} \text{ m}^{-2/3} \quad (45)$$

To compare the theoretical predictions and the experimental values, we summarize in Table 3 the values we have obtained for C_μ^2 . This table shows that the value obtained from the Karman model is closer to the experimental result than the value given by the Tatarskii model. This was predictable because it is well known that Karman model is more realistic than the Tatarskii model. The slight difference (2%) observed between the value given by the Karman model and that obtained from the experiments demonstrates the validity of the theoretical approach we have achieved for the correlation of the laser beam deflection angles.

7. CONCLUSION

In this paper, we have found a theoretical approach which is based on the geometrical optics approximation and determines the correlation function of the laser beam deflection angles, in terms of the correlation function of the refractive index fluctuations. By applying the Tatarskii model and modified Von Karman model for the turbulence spectrum, we have derived completed formulas. This enables to compute the structure coefficient of the refractive index for the hot turbulent jet

and to obtain the values of the correlation function of the laser beam deflection angles.

To validate the theoretical predictions, an experimental setup and a measurement method for the structure coefficient of the refractive index are described. A good agreement between the measured experimental value and the computed value obtained from the Karman model, demonstrates the validity of the theoretical approach. The results thus obtained will be used in subsequent works for the prediction of the temporal spectrum of the laser beam angle-of-arrival, and for the possibility of extracting information about turbulence in the hot turbulent jet considered.

ACKNOWLEDGMENT

The authors would like to thank the Reviewers for the corrections they have made to the paper and the valuable comments they have suggested for improving it.

REFERENCES

1. Tatarskii, V. I., *Wave Propagation in a Turbulent Medium*, McGraw-Hill, New York, 1961.
2. Chernov, L. A., *Wave Propagation in a Random Medium*, McGraw-Hill, New York, 1960.
3. Frehlich, R., "Simulation of laser propagation in a turbulent atmosphere," *Applied Optics*, Vol. 39, No. 3, 393–397, 2000.
4. Gomes, C. and M. Z. A. Abkadir, "Protection of naval systems against electromagnetic effect due to lightning," *Progress In Electromagnetics Research*, Vol. 113, 333–349, 2011.
5. Wei, H.-Y., Z.-S. Wu, and Q. Ma, "Log-amplitude variance of laser beam propagation on the slant path through the turbulent atmosphere," *Progress In Electromagnetics Research*, Vol. 108, 277–291, 2010.
6. Guo, J., Z. Xu, C. Qian, and W.-B. Dou, "Design of a microstrip balanced mixer for satellite communication," *Progress In Electromagnetics Research*, Vol. 115, 289–301, 2011.
7. O'Halloran, M., M. Glavin, and E. Jones, "Rotating antenna microwave imaging system for breast cancer detection," *Progress In Electromagnetics Research*, Vol. 107, 331–348, 2010.
8. Zhu, G. K. and M. Popovic, "Comparison of radar and thermoacoustic technique in microwave breast imaging," *Progress In Electromagnetics Research B*, Vol. 35, 1–14, 2011.

9. Conceição, R., M. O'Halloran, M. Glavin, and E. Jones, "Numerical modelling for ultra wideband radar breast cancer detection and classification," *Progress In Electromagnetics Research B*, Vol. 34, 145–171, 2011.
10. Alshehri, S. A., S. Khatun, A. B. Jantan, R. S. A. Raja Abdullah, R. Mahmood, and Z. Awang, "Experimental breast tumor detection using Nn-based UWB imaging," *Progress In Electromagnetics Research*, Vol. 111, 447–465, 2011.
11. Pemha, E. and E. Ngo Nyobe, "Genetic algorithm approach and experimental confirmation of a laser-based diagnostic technique for the local thermal turbulence in a hot wind tunnel jet," *Progress In Electromagnetics Research B*, Vol. 28, 325–350, 2011.
12. Tatarskii, V. I., "The effects of the turbulence atmosphere on wave propagation," US Dept. of Commerce, National Technical Information Service TT-68-50464, 1971.
13. Consortini, A. and F. Rigal, "Fractional moments and their usefulness in atmospheric laser scintillation," *Pure Applied Optic*, Vol. 7, 1013–1032, 1998.
14. Ishimaru, A., *Wave Propagation and Scattering in Random Media*, Vol. 2, Academic Press, New York, 1978.
15. Consortini, A. and K. A. O'Donnell, "Beam wandering of thin parallel beams through atmospheric turbulence," *Waves in Random Media*, Vol. 3, S11–S28, 1991.
16. Consortini, A., Y. Y. Sun, and G. Conforti, "A mixed method for measuring the inner scale of atmospheric turbulence," *Journal of Modern Optics*, Vol. 37, No. 10, 1555–1560, 1990.
17. Gulich, D., G. Funes, L. Zunino, D. G. Pérez, and M. Garavaglia, "Angle-of-arrival variance's dependence on the aperture size for indoor convective turbulence," *Optics Communications*, Vol. 277, No. 2, 241–246, 2007.
18. Alim, E. Ngo Nyobe, and E. Pemha, "Theoretical prediction and experimental validation of the angle-of-arrival probability density of a laser beam in a strong plane-flame turbulence," *Optics Communications*, Vol. 283, No. 9, 1859–1864, 2010.
19. Pemha, E., B. Gay, and A. Tailland, "Measurement of the diffusion coefficient in a heated plane airstream," *Physics of Fluids A*, Vol. 5, No. 6, 1289–1295, 1993.
20. Ngo Nyobe, E. and E. Pemha, "Shape optimization using genetic algorithms and laser beam propagation for the determination of the diffusion coefficient in a hot turbulent jet of air," *Progress In Electromagnetic Research B*, Vol. 4, 211–221, 2008.

21. Ngo Nyobe, E. and E. Pemha, "Propagation of a laser beam through a plane and free turbulent heated air flow; determination of the stochastic characteristics of the laser beam random direction and some experimental results," *Progress In Electromagnetics Research*, Vol. 53, 31–53, 2005.
22. Hona, J., E. Ngo Nyobe, and E. Pemha, "Experimental technique using an interference pattern for measuring directional fluctuations of a laser beam created by a strong thermal turbulence," *Progress In Electromagnetics Research*, Vol. 84, 289–306, 2008.
23. Born, M. and E. Wolf, *Principles of Optics: Electromagnetic Theory of Propagation, Interference and Diffraction of Light*, 7th Edition, Cambridge University Press, Cambridge, 1999.
24. Gagnaire, A. and A. Tailland, "Interferometrical setup for the study of thermic turbulence in a plane air stream," *Proceedings of SPIE*, Vol. 136, 69–73, 1997.
25. Kolmogorov, A. N., "The local structure of turbulence in incompressible viscous fluids for very large Reynolds number," *Turbulence Classic Papers on Statistical Theory*, S. K. Friedlander and L. Topper, Eds., 151–155, Wiley-Interscience, New York, 1961.
26. Abramowitz, A. and I. A. Stegun, *A Handbook of Mathematical Functions*, Dover, New York, 1964.
27. Davis, P. J. and P. Rabinowitz, *Methods of Numerical Integration*, Academic Press, New York, 1975.
28. Weiss, A., "Determination of thermal stratification and turbulence of the atmospheric surface layer over various types of terrain by optical scintillometry," Ph.D. Thesis, ETH No. 14514, Swiss Federal Institute of Technology, Zurich, 2002.
29. Meijninger, W. M. L., "Surface fluxes over natural landscapes using scintillometry," Ph.D. Thesis, Wageningen University, The Netherlands, 2003.